Measurement Standards for Optically Active Coatings to Improve Shipboard Tank Preservation

Maria Nadal* and C. Cameron Miller
National Institute of Standards and Technology
100 Bureau Drive, mail stop 8442
Gaithersburg, MD 20899-8442
Phone: 301-975-4632
Fax: 301-840-8551
maria.nadal@nist.gov and c.miller@nist.gov

Richard Harold
Color and Appearance Consulting, LLC
P. O. Box 607
Herndon, VA

Paul Gossen
National Surface Treatment Center
401 Industry Road, Suite 500
Louisville, KY 40208

*Corresponding author

Word count:5400

Abstract: The cost of corrosion control to the Department of Defense (DOD) is estimated to be $20B/yr. Eliminating coating defects during the coating application job is the key to extending coating service life. Fluorescent coatings containing additives that fluoresce under violet light are commercially available. NAVSEA requires a specification and test method for this fluorescent coating so that it can be specified in Navy coating contracts. The objective of the project is to develop a tolerance budget so ASTM committee E12 on Color and Appearance will have the knowledge to develop an ASTM test method characterizing the fluorescent optical property. Presented is the measurement equation, the experimental and simulation details, along with the analysis to determine sensitivity coefficients to develop a tolerance budget.

Keywords: luminance ratio, optically active coatings, tolerances, uncertainty budget

1. Introduction

The cost of corrosion control to the Department of Defense (DOD) is estimated to be \$20B/yr. For example, the U.S. Navy spends about \$2.4B/yr on corrosion control for shipboard tanks like seawater ballast tanks, potable water tanks, and fuel tanks. Coating shipboard tanks is the Fleet's #1 maintenance cost, and extending coating service life is the core strategy to lowering this cost. Eliminating coating defects during the coating application job is the key to extending coating service life. Fluorescent coatings containing additives that fluoresce under violet light are commercially available. Under violet light inspection areas where coatings have developed holidays, coverage is incomplete, and corrosion under the coating is revealed. With the fluorescent additives in the primer, bright regions tend to indicate higher than expected dry film thickness. Dull or low luminosity indicates lower than expected dry film thickness. After applying a topcoat, the fluorescence should disappear. A region where fluorescence is still present indicates insufficient topcoat thickness. The average worker with 20/20 vision can usually locate a defect 0.5 mm in size. With the optically active coatings the same worker can locate defects 0.1 mm in size or smaller in low-light conditions.[1]

Naval Sea Systems Command (NAVSEA) has demonstrated that this fluorescent coating technology improves the quality of tank coating applications in the field. NAVSEA requires a specification and test method for this fluorescent coating so that it can be specified in Navy coating contracts. The objective of the project is to develop a tolerance budget so ASTM committee E12 on Color and Appearance will have the knowledge to develop an ASTM test method characterizing the fluorescent optical property. With an ASTM test method the U.S. Navy can work with ASTM to create a specification for fluorescent primers which will save the DOD billions on corrosion control for shipboard tanks and other military applications in harsh environments.

2. Measurement equation

The first step in developing ASTM test method E2630-08 "Standard Test Method for Luminance Ratio of a Fluorescent Specimen using a Narrow Band Source"[2] was to establish the measurement equation and then list the uncertainty components that may influence the measurement result. The luminance ratio, for this measurement, is defined as the luminance of the sample under a given narrow band source peaked at 405 nm divided by the luminance of a 25 % reflecting Lambertian diffuser under the same 405 nm narrow band source. The following equation models the luminance ratio

$$R_L^B = \frac{L^B}{L_P^B}, \tag{1}$$

where $R_L{}^B$ is the luminance ratio, L^B is the sample luminance, and $L_P{}^B$ is the reference luminance. (*B* represents a quantity for narrow band illumination) Figure 1 shows a schematic of the measurement setup. The fluorescent sample luminance is the luminance meter signal divided by the responsivity of the luminance meter for the spectrum of light emitted from the sample, which is different than the 405 nm source. The following equation models the sample luminance

$$L^B = \frac{(s - s_d)}{r \cdot F}, \tag{2}$$

where L^B is the fluorescent sample luminance, s is the luminance meter signal, s_d is the luminance meter signal with the 405 nm source blocked, r is the responsivity of the luminance meter and F is the spectral mismatch correction factor of the luminance meter for the spectrum of light emitted from the sample. The light from the sample consist of 405 nm light reflected from the sample and fluorescence emitted from the sample.

The reference luminance is the luminance meter signal divided by the responsivity of the luminance meter for the 405 nm source multiplied by the 25 % reflecting Lambertian diffuser divided by the calibrated reflectance of the non-fluorescing standard under the 405 nm source. The following equation models the reference luminance

$$L_P^B = \frac{(s_P - s_{P,d})}{r \cdot F_P} \cdot \frac{0.25}{\rho^B}, \tag{3}$$

where $L_P{}^B$ is the reference luminance, s_P is the luminance meter signal, $s_{P,d}$ is the luminance meter signal with the 405 nm source blocked, r is the responsivity of the luminance meter, F_P is the spectral mismatch correction factor of the luminance meter for the spectrum of light reflected from the reference sample, and ρ^B is the reflectance of the non-fluorescing standard under the 405 nm source. (P represents a quantity for the non-fluorescing standard.) Substituting eq. (2) and eq. (3) into eq. (1) results in

$$R_L^B = \frac{(s - s_d)}{(s_P - s_{P,d})} \cdot \frac{F_P}{F} \cdot \frac{\rho^B}{0.25} \cdot C_f\,. \tag{4}$$

Notice that the absolute responsivity of the luminance meter cancels. The additional term, C_f, stands for all other factors that contribute uncertainty to the measurement. The magnitude of C_f is unity because there is no knowledge of the magnitude of the factors, just the uncertainty they contribute. All of these uncertainty components including the terms in eq. (4) are listed below.

s_P	– non-fluorescing standard signal
$s_{P,d}$	– non-fluorescing standard dark signal
s	– fluorescing sample signal
s_d	– fluorescing sample dark signal
F_P	– spectral mismatch correction of responsivity non-fluorescing standard signal
F	– spectral mismatch correction of responsivity fluorescing sample signal
ρ^B	– luminance reflectance of calibrated non-fluorescing standard

λ^B – excitation wavelength dependence
$\Delta\lambda^B$ – illumination bandwidth dependence
λ_S – spectral out-of-band light (fluorescence from source)
S – out-of-band stray light (inside detector)
L – linearity of the detector
S_f – Out-of-field sensitivity of the luminance meter
c_s – voltmeter calibration
ϕ_P – incident angle of light on non-fluorescing standard
ϕ – incident angle of light on fluorescing sample
θ_P – viewing angle of light from non-fluorescing standard
θ – viewing angle of light from fluorescing sample
U_L – uniformity of the light source
U_P – uniformity of the non-fluorescing standard material
U – uniformity of the fluorescing sample material
U_r – uniformity of the detector responsivity
T_P – temperature dependence of the non-fluorescing standard material
T – temperature dependence of the fluorescing sample material
T_r – temperature dependence of the luminance meter responsivity
P_P – polarization dependencies of the non-fluorescing standard material
P – polarization dependencies of the fluorescing sample material
P_r – polarization dependencies of the luminance meter

ASTM has a guidance document D4536-84 (2002): "Standard Practice for Establishing Consistent Test Method Tolerances" that describes the method of setting parameter tolerances for a test method.[3] The relationship of a determination tolerance (the expected range of the result) to the measurement tolerances (the acceptable range of each parameter) is determined by

$$\frac{\Delta R^2}{2} = \sum_{i=1}^{q}\left(\frac{\partial R}{\partial X_i}\right)^2 \Delta X_i^2 , \quad (5)$$

where X_i is a measurement value, ΔX_i is the specified measurement tolerance for that parameter, R is the determination value, ΔR is the determination tolerance and $\partial R/\partial X_i$ is the sensitivity coefficient for the determination value with respect to the measurement parameter. The measurement value is the mean of a uniform distribution and measurement tolerance is the interval or range of the uniform distribution. The determination value has a 98.6 % probability of falling in the determination tolerance based on assumptions and simplifications in Eq. (5).

Each of these components or measurement parameters through experiments or simulations was analyzed to determine the sensitivity coefficients. The following sections provide the experimental details, results and analysis to determine the sensitivity coefficients. The ASTM E12 committee was required to select the measurement tolerances, calculate the determination tolerance and agree upon an acceptable magnitude of the determination tolerance. The tolerance budget brings all the results together in a tabular summary.

3. Experimental details

Two experimental configurations were used to collect the required data. One configuration is based on several excitation wavelengths with stray-light corrected spectral detection. The spectral data is used in simulations discussed in the analysis section. The second configuration is based on a single illumination wavelength at 405 nm with photopic detection corrected for spectral mismatch. The photopic detection scheme was used to determine the sensitivity of many environmental conditions.

3.1. Spectral measurements

The spectral distribution of the reflected and emitted light from a non-fluorescent standard and a fluorescing sample illuminated by different wavelengths of narrow band, 8 nm full width half maximum (FWHM), light was collected. The excitation light was generated by a 1000 W Xe arc source reflected off a heat transmitting mirror through a lens to form a collimated beam. The Xe arc source has a feedback control to stabilize the light output. The beam was baffled to reduce spatial stray light and wavelengths were selected with interference filters. The incident light is normal to the surface. The reflected and emitted light was collected by a calibrated stray-light corrected CCD spectrometer.[4] The input optic was a quartz fiber optic bundle position at 45° with respect to the surface normal. The acceptance angle of the fiber optic is larger than the incident beam spot on the non-fluorescing standard or fluorescing sample.

3.2. Photometric measurements

The photometric measurements were conducted using a 405 nm temperature stabilized LED source and a high quality luminance meter. Figure 2 is a schematic of the LED source. A 5 W LED package with a peak wavelength of 405.0 nm ± 0.1 nm is attached to a thermoelectric cooler to maintain a constant heat sink temperature. The full width half maximum of the emitted light is 16.3 nm ± 0.1 nm. A silica lens images the emitted light from the LED into a nearly collimated uniform beam with a spot diameter of 75 mm. At a distance of 50 cm the irradiance is 32 W/m^2. The LED source is filtered with a blue-green filter to eliminate the fluorescence within the system. The luminance meter has four fixed fields of view, 0.1°, 0.3°, 1.0° and 3.0° and is photopic filter based. The radiance responsivity of the luminance meter has been determined to allow for spectral mismatch corrections. The incident light is normal to the surface and the luminance meter is positioned 45° to the surface normal. The luminance meter was set at a distance where the field of view under views the illuminated spot.

4. Results & analysis

The following sections describe the results and analysis of experiments and simulations that were used to determine sensitivity coefficients for the uncertainty components listed previously.

4.1. Excitation wavelength

Figure 3 shows the stray light corrected spectra for the non-fluorescent reference standard illuminated by several wavelengths of the filtered Xe source was measured. These spectra were used to determine the sensitivity coefficient for excitation wavelength with respect to the luminance ratio. The fraction of radiometric power in the spectra more than 25 nm red shifted from the peak was less than 0.10 %, which demonstrates the lack of fluorescence. Figure 4 shows the stray light corrected spectra collected for a fluorescing test sample. As the peak intensity shifts towards the ultraviolet, the absorption increases. Figure 5 is the same data as Figure 4 expanded by a factor of 25 along the axis of intensity. The fluorescence is evident at this resolution.

The luminance ratio from the spectral data is determined by

$$R_L^B = \frac{\int S_B(\lambda)V(\lambda)\mathrm{d}\lambda}{\int S_P(\lambda)V(\lambda)\mathrm{d}\lambda} \cdot \frac{\rho^B}{0.25} \tag{6}$$

where $S_B(\lambda)$ is the reflected and emitted spectrum of the fluorescing sample, $S_P(\lambda)$ is the reflected spectrum of the non-fluorescent standard, $V(\lambda)$ is the luminous efficacy function and ρ^B is the reflectance of the non-fluorescent standard under the 405 nm source. Equation 6 for spectral measurements is the same as eq. (4) for photopic measurements. The results of the calculation are shown in Figure 6. By fitting a polynomial to the data, taking the derivative with respect to the excitation wavelength, and evaluating the derivative at 405 nm, a sensitivity coefficient of -10 %/nm is determined. This sensitivity coefficient is used in the tolerance budget described later.

4.2. Illumination bandwidth

The sensitivity coefficient of the illumination bandwidth with respect to the luminance ratio is determined by running simulations on the data collected in the excitation wavelength experiments. To calculate the percent change in luminance ratio the curve in Figure 6 is multiplied by a Gaussian distribution centered at 405 nm and with a FWHM ranging from 1 to 24 nm. The resulting curve is integrated to determine the area under each curve. All of the calculated areas are divided by the area determined for a Gaussian distribution with a FWHM of 8 nm. The percent change in luminance ratio is plotted versus illumination bandwidth as shown in Figure 7 and fitted by a polynomial. The derivative of the polynomial is determined and evaluated at 16 nm which is the typical bandwidth for a single chip 405 nm LED. The sensitivity coefficient for illumination bandwidth with respect to the luminance ratio for this fluorescing sample was determined to be 2.4 %/nm evaluated at a bandwidth of 16 nm. The assumption for this simulation is that the luminance ratio curve in Figure 6 is the result of illumination with zero bandwidth. Since the tolerance analysis is only concerned with approximating the sensitivity coefficient and the percent change in luminance ratio from 8 nm to 0 nm bandwidth is -3.5 %, the assumption is acceptable.

4.3. Out of band stray light from the illumination source

A potential source of significant error is the out-of-band stray light from the illumination source. When illuminating the sample the assumption is that the spectral distribution of the illumination source will be peaked at 405 nm with a FWHM of 16 nm. However, 405 nm light can cause undesired fluorescence within the illumination package. Figure 8 shows the spectral irradiance distribution for a typical 405 nm LED based source as a solid line. The dashed curve has been multiplied by a factor of 1000 to show the small fluorescence which originates within the LED package. The fraction of light caused by fluorescence (wavelength > 500 nm) is 0.34 % of the total light from the LED source illuminating the sample. This small amount of light is enhanced by the spectral responsivity of the luminance meter. The 0.34 % (radiometric) of light due to the fluorescence accounts for 55.1 % of the luminance signal from the non-fluorescing standard. The luminance ratio dependency on the out of band stray light for the source is given by

$$R_L^B \approx \frac{A+x}{B+x}, \tag{7}$$

where A is the luminance signal from the fluorescing sample, B is the luminance signal from the non-fluorescent standard, and x is the luminance signal from the source fluorescence. The error in the luminance ratio for the fluorescing sample described in Figure 4 with this light source is -53 %. A blue-green filter was used to reduce the fluorescence to a radiometric contribution of 0.003 % and a photometric contribution of 1.4 %. The error in the luminance ratio is reduced to -1.4 %. Several sources with and without several different filters were measured to determine the effect of source fluorescence on the luminance ratio. The results plotted in Figure 9 were fit with a polynomial and a sensitivity coefficient of -341 %/ (radiometric % of fluorescence) was determined at a radiometric fluorescence contribution of 0.01 %.

4.4. Spectral mismatch

A potentially significant source of error in photometric measurements is spectral mismatch. Spectral mismatch is the difference in spectral responsivity of a real luminance meter compared to the luminous efficacy function, $V(\lambda)$. A spectral mismatch correction factor is calculated according to

$$F = \frac{\int_\lambda S_A(\lambda)s(\lambda)\mathrm{d}\lambda}{\int_\lambda S_A(\lambda)V(\lambda)\mathrm{d}\lambda} \cdot \frac{\int_\lambda S_X(\lambda)V(\lambda)\mathrm{d}\lambda}{\int_\lambda S_X(\lambda)s(\lambda)\mathrm{d}\lambda} \tag{8}$$

where $S_A(\lambda)$ is the relative spectral power distribution of CIE Illuminant A (the calibration source for the luminance meter), $S_X(\lambda)$ is the relative spectral power distribution of the light being measured, $s(\lambda)$ is the spectral responsivity of the luminance meter, $V(\lambda)$ is the luminous efficacy function. Figure 10 shows these curves for a high quality luminance meter, a non-fluorescing standard and a fluorescing sample. The spectral mismatch correction factor calculated for the measurement of the non-fluorescing standard is 0.321; therefore, this luminance meter is measuring a signal three times the actual luminance. The spectral mismatch correction factor calculated for the measurement of the fluorescing sample is 0.984 which gives an error of 1.6 %. To determine the sensitivity coefficient for luminance ratio with respect to spectral mismatch correction factor, the sensitivity coefficient for spectral mismatch correction factor with respect to wavelength must be evaluated. The spectral mismatch correction factor was calculated for the non-fluorescing standard by simulating the illuminating spectral power distribution every 1 nm. The results are shown in Figure 11. The spectral mismatch correction factor for the fluorescing sample was calculated based on the spectral data collected in Figure 4. These results are also shown in Figure 11. The results are fit to a polynomial, the derivative is determine and evaluated at 405 nm. The sensitivity coefficient of the spectral mismatch correction factor with respect to wavelength for the non-fluorescing standard was determined to be -2.4 %/nm at 405 nm and for the fluorescing sample was determined to be -0.6 %/nm at 405 nm. These sensitivity coefficients are the spectral mismatch correction factor with respect to the excitation wavelength. Using the chain rule the sensitivity coefficient for the luminance ratio with respect to the excitation wavelength can be determined. This is required since the spectral mismatch correction factor is dependent on the excitation wavelength. By taking the partial derivative of eq. (4) with respect to the spectral mismatch correction factors and multiplying by the experimental determined sensitivity coefficients as shown below

$$\frac{\partial R_L^B}{\partial \lambda} = \frac{\partial R_L^B}{\partial F_P}\frac{\partial F_P}{\partial \lambda} = \frac{R_L^B}{F_P}(-2.4 \,{}^{\%}\!/_{nm}) \tag{9}$$

the sensitivity coefficient required for the tolerance budget is calculated. The sensitivity coefficient is dependent on the excitation wavelength, not the spectral mismatch correction factor directly. The spectral mismatch correction factor needs to be considered when deciding on the final excitation wavelength tolerance.

4.5. Out-of-band stray light in the spectroradiometer

An experimental approach used to avoid spectral mismatch is to use a spectroradiometer to measure the spectral radiance. Spectroradiometers have many factors in common with photometers such as linearity and sensistivity, but the most significant factor not in common is out-of-band straylight. The out-of-band straylight is a signal that is caused by light that is the incorrect wavelength. Figure 12 shows an example of the spectral irradiance distribution measured from the non-fluorescing standard using a single grating CCD spectrometer. A reasonably good single grating CCD spectrometer can have stray light rejection of 10^4. The second curve is the measured spectral irradiance distribution corrected for stray light. The stray light correction increases the rejection to 10^5. This factor of ten is significant because of the luminous efficacy function weighting. Figure 13 shows the spectral irradiance distributions multiplied by the luminous efficacy function. The area under the non-corrected weighted curve is comparable to the area under the 405 nm reflected peak. Figure 14 shows the non-corrected and corrected spectral irradiance distribution for the fluorescing sample. The stray light is almost insignificant because of the fluorescing light level. Using the curves in Figure 12 and Figure 14 to calculate the luminance ratio shows that the error due to stray light is 45 %. The stray light level of 10^3 was simulated by multiplying the non-corrected signal above 425 nm by 10. The stray light level of 10^6 was simulated by dividing the corrected signal above 425 nm by 10. The luminance ratios were calculated and fit to a polynomial versus the stray light rejection level. The derivative was taken and evaluated at 10^5 to give a sensitivity coefficient of -511007 %/(stray light rejection level).

4.6. Geometrical characterization

Depending on the optical properties of the test sample, the result may be very sensitivity to the geometrical configuration of the measurement. Since the non-fluorescing standard is a near-ideal diffuse material and fluorescence from the fluorescing sample emits in all directions, the expectation for geometrical sensitivity is low. The incident angle sensitivity was measured by changing the incident angle to the non-fluorescing standard and the fluorescing sample from -10° to 10° by steps of 2.5° while maintaining the 45° viewing angle from the new incident angle. Figure 15 shows the percent change on the luminance ratio with respect to the incident angle. The result was fit to a polynomial; the derivative was taken and evaluated at 0° incident angle. The sensitivity coefficient was determined to be -0.225 %/degree. The viewing angle sensitivity was determined by fixing the incident angle at 0° and changing the viewing angle from 40° to 50° by steps of 2.5°. Figure 16 shows the percent change on the luminance ratio with respect to the viewing angle. The resulting sensitivity coefficient was determined to be 0.067 %/degree.

5. Tolerance budget

The final product of this work is a tolerance budget that is used to decide appropriate tolerances for the ASTM test method. Table 1 is the tolerance budget for the determination of luminance ratio for a fluorescing sample compared to a non-fluorescing standard using a photopic filter based luminance meter and a 405 nm narrow band source. In the budget, each component requiring a tolerance has been listed along with a typical value for the measurement. Each sensitivity coefficient has been changed from a relative number to an absolute number by multiplying the final luminance ratio value. For the four signal components, the sensitivity coefficient is the partial derivative of equation 4 with respect to the signal component. The contribution is the sensitivity coefficient square times the tolerance squared which is what is summed in equation 5. The predicted precision or determination tolerance is the square root of two times the sum of the contributions. The determination value or luminance ratio was calculated using equation 4 where all of the components not specifically listed in equation 4 are factors set to unity in the term C_f. Therefore,

$$C_f = \lambda_B \cdot \Delta\lambda_B \cdot \lambda_s \cdot \phi \cdot \theta \cdot L \cdot O \cdot c_s = 1 \,. \tag{10}$$

The relative contribution values were calculated by taking the square root of the contribution times 2 divided by the determination value.

Measurement tolerances were chosen based on the final contribution to the overall budget or based on what is a realistic value for the technology presently available. The largest source contributing to the determination tolerance is the measurement tolerance for the excitation wavelength. By fixing the excitation wavelength of the source to 405 nm ± 1 nm (ΔX_i = 2 nm) the minimum determination tolerance was set at 28 % or a range of ± 14 % about the determination value. The ASTM committee decided that a measurement tolerance smaller than 2 nm was putting an undue burden on the laboratories, considering the expected usage of the test method. The measurement tolerance with the next largest impact is the illumination bandwidth. The ASTM committee wanted to allow many source technologies to be used for the test method including LEDs and grating monochromator systems; therefore, the shape of the spectral distribution shall be triangular, Gaussian or isosceles trapezoidal where the width of the peak shall be less than one sixth the size of the base and it shall have a full width half maximum of 16 nm (± 2 nm). The measurement tolerance of 4 nm for the illumination bandwidth results in a 14 % contribution to the determination tolerance. The other measurement tolerances were chosen to not place a significant burden on the laboratories, such as setting the display resolution to 100:1 for the reference and sample signal, without significantly increasing the determination tolerance. The tolerance for the luminous reflectance of the non-fluorescing standard is the expectation of the uncertainty for calibrations done at the National Institute of Standards and Technology (NIST).

Table 2 is the tolerance budget for the determination of luminance ratio for a fluorescing sample compared to a non-fluorescing standard using a spectroradiometer based luminance meter and a 405 nm narrow band source. The only difference is the spectral mismatch correction factors for the non-fluorescing standard and fluorescing sample are removed and the component due to the stray light in the detection system has been added. Coincidentally the contribution from the spectral mismatch correction factors is on the same order as the stray light component.

The sensitivity coefficients for components dealing with temperature, uniformity, and polarization are currently topics of research at NIST.

6. Tolerance versus uncertainty budget

A tolerance budget is developed in the preparation of a test method. It gives guidance on the expectation a laboratory can have if the prescribed tolerances are followed. In this example, if a laboratory just follows the prescribed tolerances the expectation is that there is a 98.6 % probability the determined value will fall within a range that is ± 16.5 % of the true value.

With additional work a laboratory can determine an uncertainty budget where there is a 95 % probability that the true value falls within a range centered at the determined value. The uncertainty budget is composed of the same components in the tolerance budget and even uses the same sensitivity coefficients. According to the Guide to Uncertainty of Measurements[5] or NIST Technical Note 1297[6], the combine uncertainty is calculated by,

$$u_c^2(y) = \sum_{i=1}^{N}\left[\frac{\partial f}{\partial x_i}\right]^2 u^2(x_i) + 2\sum_{i=1}^{N-1}\sum_{j=i+1}^{N}\frac{\partial f}{\partial x_i}\frac{\partial f}{\partial x_j}u(x_i)u(x_j)r(x_i,x_j)\,. \qquad (11)$$

where $u_c(y)$ is the combine uncertainty, $\partial f/\partial x_i$ is the sensitivity coefficient, $u(x_i)$ is the standard deviation of the component, and $r(x_i,x_j)$ is the correlation coefficient. For this analysis the correlation coefficient has been set to zero for all the components. This is currently a topic of research at NIST. The expanded uncertainty is reported with the measurement result which is the combine uncertainty multiplied by a coverage factor, k, in this case $k = 2$.

Table 3 is the uncertainty budget for the NIST calibration of a fluorescing sample for luminance ratio. To achieve a low uncertainty additional characterization is required. The luminance meter has been calibrated for spectral radiance responsivity at the NIST Spectral Irradiance and Radiance Calibration using Uniform Sources (SIRCUS)facility.[7] The SIRCUS facility is a laser based facility that allows the calibration of the luminance meter for very low wavelength uncertainty and responsivity uncertainty. Having this data allows the spectral mismatch correction factors to be calculated with the lowest possible uncertainty. The 405 nm narrow band source is a temperature controlled single chip LED based source. The LEDs were initially screened to find an LED that under typical operating temperatures emitted very close to a peak of 405 nm. By controlling the heat sink temperature the LED peak wavelength is shift to 405.0 nm ± 0.2 nm ($k = 2$). To determine the wavelength a spectroradiometer calibrated to a wavelength scale of 0.05 nm is required. The remaining components were characterized to determine the standard deviation about the value, instead of just allowing the measurement of the component to fall within a tolerance. By applying equation 11 with the correlation coefficients set to zero an expanded uncertainty of 1.7 % ($k = 2$) for luminance ratio is achievable at NIST. Typical laboratories would probably expect an expanded uncertainty of 5 % to 6 % ($k = 2$) for luminance ratio which is much less than the tolerance budget would imply.

Acknowledgments

The authors would like to acknowledge the contributions from the ASTM E12 committee on Color and Appearance. In addition, the authors would like to thank the Coordination Calibration Group for their financial support.

Table 1 Tolerance budget for luminance ratio using a photopic filter based luminance meter

Component	Symbol	Value	ΔX_i	$\partial R_L^B/\partial X_i$	Contribution	%
Sample signal	s	4.212 V	0.04 V	3.62 V^{-1}	0.0209	1.3
Sample dark signal	s_d	0.000 V	0.04 V	-3.62 V^{-1}	0.0209	1.3
Reference signal	s_P	0.3500 V	0.0035 V	-43.52 V^{-1}	0.0232	1.4
Reference dark signal	$s_{P,d}$	0.0000 V	0.0035 V	43.52 V^{-1}	0.0232	1.4
Spectral mismatch - sample	F	0.984	2 nm	0.091 nm^{-1}	0.0334	1.7
Spectral mismatch - reference	F_P	0.321	2 nm	-0.366 nm^{-1}	0.5346	6.8
Standard luminance reflectance	ρ_B	0.97	0.003	15.70	0.0022	0.4
Excitation wavelength	λ_B	1	2 nm	-1.52 nm^{-1}	9.2808	28.3
Illumination bandwidth	$\Delta\lambda_B$	1	4 nm	0.37 nm^{-1}	2.1383	13.6
Spectral out-of-band light	λ_s	1	0.01	-51.91	0.2695	4.8
Illumination angle	ϕ	1	2°	-0.0343 /°	0.0047	0.6
Viewing angle	θ	1	4°	0.0102 /°	0.0017	0.4
Linearity of detector	L	1	0.01	15.23	0.0232	1.4
Out-of-field sensitivity	O	1	0.005	15.23	0.0058	0.7
Voltmeter calibration	c_S	1	0.001	15.23	0.0002	0.1
Luminance Ratio	$\boldsymbol{R_L^B}$	**15.23**	**Predicted precision**		**4.98**	
			Relative precision		**33 %**	

Table 2 Tolerance budget for luminance ratio using a spectroradiometer based luminance meter

Component	Symbol	Value	ΔX_i	$\partial R_L^B / \partial X_i$	Contribution	%
Sample signal	s	4.280 V	0.04 V	3.56 V^{-1}	0.0209	1.3
Sample dark signal	s_d	0.000 V	0.04 V	-3.56 V^{-1}	0.0209	1.3
Reference signal	s_P	1.090 V	0.01 V	-13.98 V^{-1}	0.0232	1.3
Reference dark signal	$s_{P,d}$	0.0000 V	0.01 V	13.98 V^{-1}	0.0232	1.3
Standard luminance reflectance	ρ_B	0.97	0.003	15.70	0.0022	0.4
Excitation wavelength	λ_B		2 nm	-1.52 nm^{-1}	9.2808	28.3
Illumination bandwidth	$\Delta\lambda_B$	1	4 nm	0.37 nm^{-1}	2.1383	13.6
Spectral out-of-band light	λ_s	1	0.01	-51.92	0.2695	4.8
Out-of-band stray light	S	1	1×10^{-5}	-7.78×10^{4}	0.6060	7.2
Illumination angle	ϕ	1	2°	-0.0343 /°	0.0047	0.6
Viewing angle	θ	1	4°	0.0102 /°	0.0017	0.4
Linearity of detector	L	1	0.01	15.23	0.0232	1.4
Out-of-field sensitivity	O	1	0.005	15.23	0.0058	0.7
Voltmeter calibration	c_S	1	0.001	15.23	0.0002	0.1
Luminance Ratio	R_L^B	**15.23**	**Predicted precision**		**4.98**	
			Relative precision		**33 %**	

Table 3 Uncertainty budget for luminance ratio using NIST facilities

Component	Symbol	Value	ΔX_i	$\partial R_L^B / \partial X_i$	Contribution	%
Sample signal	s	4.2120 V	0.0005 V	3.62 V^{-1}	0.000003	0.01
Sample dark signal	s_d	0.0001 V	0.0005 V	-3.62 V^{-1}	0.000003	0.01
Reference signal	s_P	0.3500 V	0.0001 V	-43.52 V^{-1}	0.000019	0.03
Reference dark signal	$s_{P,d}$	0.0000 V	0.0001 V	43.52 V^{-1}	0.000019	0.03
Spectral mismatch - sample	F	0.984	0.001	-15.48	0.000240	0.10
Spectral mismatch - reference	F_P	0.321	0.001	47.45	0.002252	0.31
Standard luminance reflectance	ρ_B	0.9700	0.0025	15.70	0.001541	0.26
Excitation wavelength	λ_B	1	0.1 nm	-1.52 nm^{-1}	0.023202	1.00
Illumination bandwidth	$\Delta\lambda_B$	1	0.05 nm	0.37 nm^{-1}	0.000334	0.12
Spectral out-of-band light	λ_s	1	0.0005	-51.91	0.000674	0.17
Illumination angle	ϕ	1	0.1°	-0.0343 /°	0.000012	0.02
Viewing angle	θ	1	0.1°	0.0102 /°	0.000001	0.01
Linearity of detector	L	1	0.0005	15.23	0.000058	0.05
Out-of-field sensitivity	O	1	0.0005	15.23	0.000058	0.05
Voltmeter calibration	c_S	1	0.00005	15.23	0.000001	0.01
Luminance Ratio	R_L^B	**15.23**		**Combined unc.**	**0.17**	
Relative expanded uncertainty		**2.2 %**		**Rel. combined unc.**	**1.1%**	

Figure caption(s)

Figure 1 – Schematic of the measurement setup

Figure 2 – Schematic of the 405 nm LED source.

Figure 3 - Stray light corrected spectra for the non-fluorescent reference standard illuminated by several wavelengths of the filtered Xe source.

Figure 4 – The stray light corrected spectra collected for a fluorescing test sample illuminated by several wavelengths of the filtered Xe source.

Figure 5 – The stray light corrected spectra collected for a fluorescing test sample illuminated by several wavelengths of the filtered Xe source with the intensity axis expanded by a factor of 25.

Figure 6 – Luminance ratio for the fluorescing test sample at several excitation wavelengths.

Figure 7 – Percent change in luminance ratio with respect to the bandwidth of the illumination source.

Figure 8 - The spectral irradiance distribution for a typical 405 nm LED based source. The dashed curve is the same curve multiplied by a factor of 1000.

Figure 9 – Percent change in luminance ratio versus the radiometric percent of fluorescence from various 405 nm sources.

Figure 10 – The luminance meter responsivity, $s(\lambda)$ and the luminous efficacy function, $V(\lambda)$, compared to the relative spectral power distribution at an illumination wavelength of 405 nm of the fluorescing sample, $S_B(\lambda)$, the non-fluorescing standard, $S_P(\lambda)$,and CIE Illuminant A, $S_A(\lambda)$.

Figure 11 – Percent change in spectral mismatch correction factor for the non-fluorescing standard (squares) and for the fluorescing sample (circles) versus wavelength.

Figure 12 - The spectral irradiance distribution measured from the non-fluorescing standard (solid line) using a single grating CCD spectrometer and corrected for stray light (dashed line) plotted on a logarithmic scale.

Figure 13 – The spectral irradiance distributions from Figure 12 multiplied by the luminous efficacy function and plotted on a linear scale.

Figure 14 – The non-corrected and stray light corrected spectral irradiance distribution for the fluorescing sample.

Figure 15 – The percent change on the luminance ratio with respect to the incident angle fit to a polynomial.

Figure 16 - The percent change on the luminance ratio with respect to the viewing angle fit to a polynomial.

References

[1] Jacobson, G., Army Uses Smart Technology to Fight Corrosion at Fort Bragg, Volume 2, Number 2, Summer 2006. CorrDefense Online Magazine. http://corrdefense.nace.org/index.asp

[2] ASTM E2630-08, "Standard Test Method for Luminance Ratio of a Fluorescent Specimen using a Narrow Band Source," ASTM International, West Conshohoken, PA. (2008).

[3] ASTM D4536-84 (2002): "Standard Practice for Establishing Consistent Test Method Tolerances," ASTM International, West Conshohoken, PA. (2002).

[4] Zong Y., Brown S. W., Johnson B. C., Lykke K. R., Ohno Y., A Simple Stray-light Correction Method for Array Spectroradiometers, *Applied Optics*, **45**, pp. 1111 – 1119. (2006).

[5] Guide to the Expression of Uncertainty in Measurement, International Organization for Standardization, 1995.

[6] Taylor, B.N. and Kuyatt, C.E., Guidelines for Evaluating and Expressing the Uncertainty of NIST Measurement Results, NIST Technical Note 1297, 1994. Available for download at http://physics.nist.gov/Document/tn1297.pdf

[7] Brown, S.W., Eppeldauer, G.P., and Lykke, K.R., NIST facility for spectral irradiance and radiance response calibrations with a uniform source, *Metrologia* 37, 579 (2000).

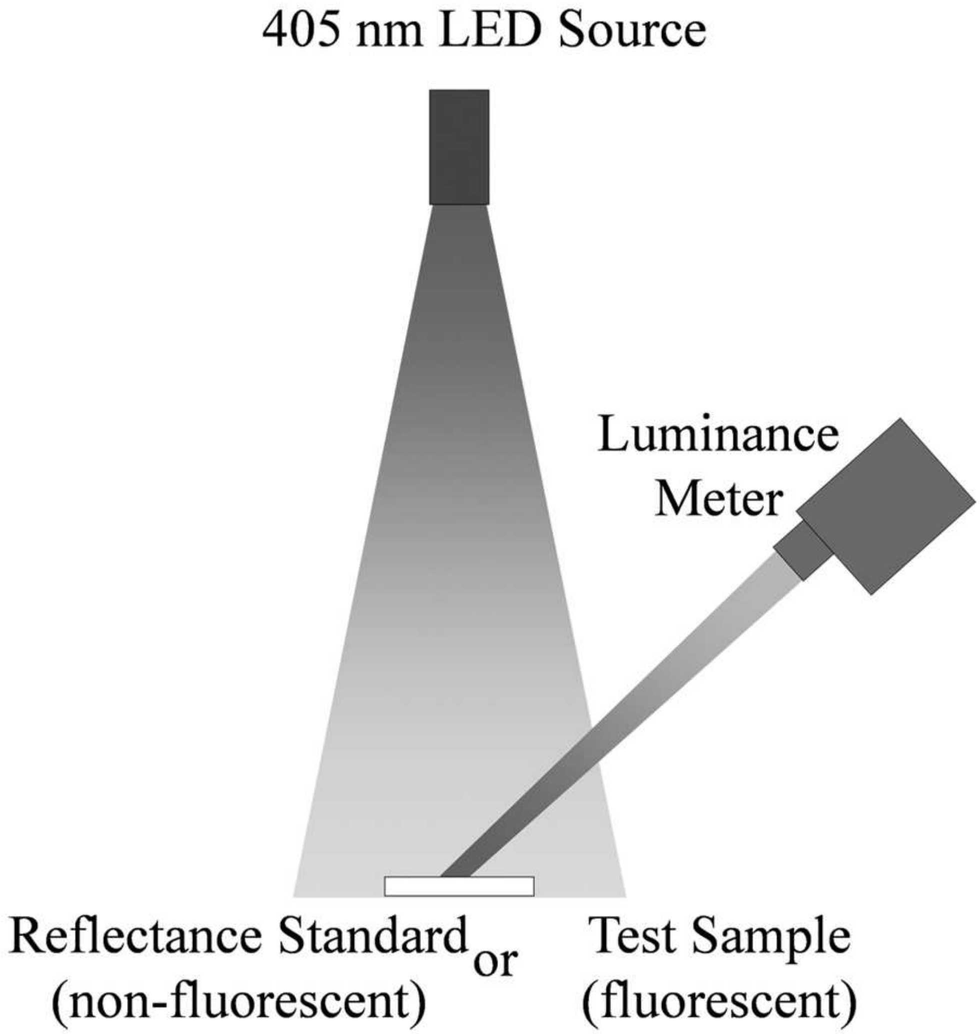

78x82mm (300 x 300 DPI)

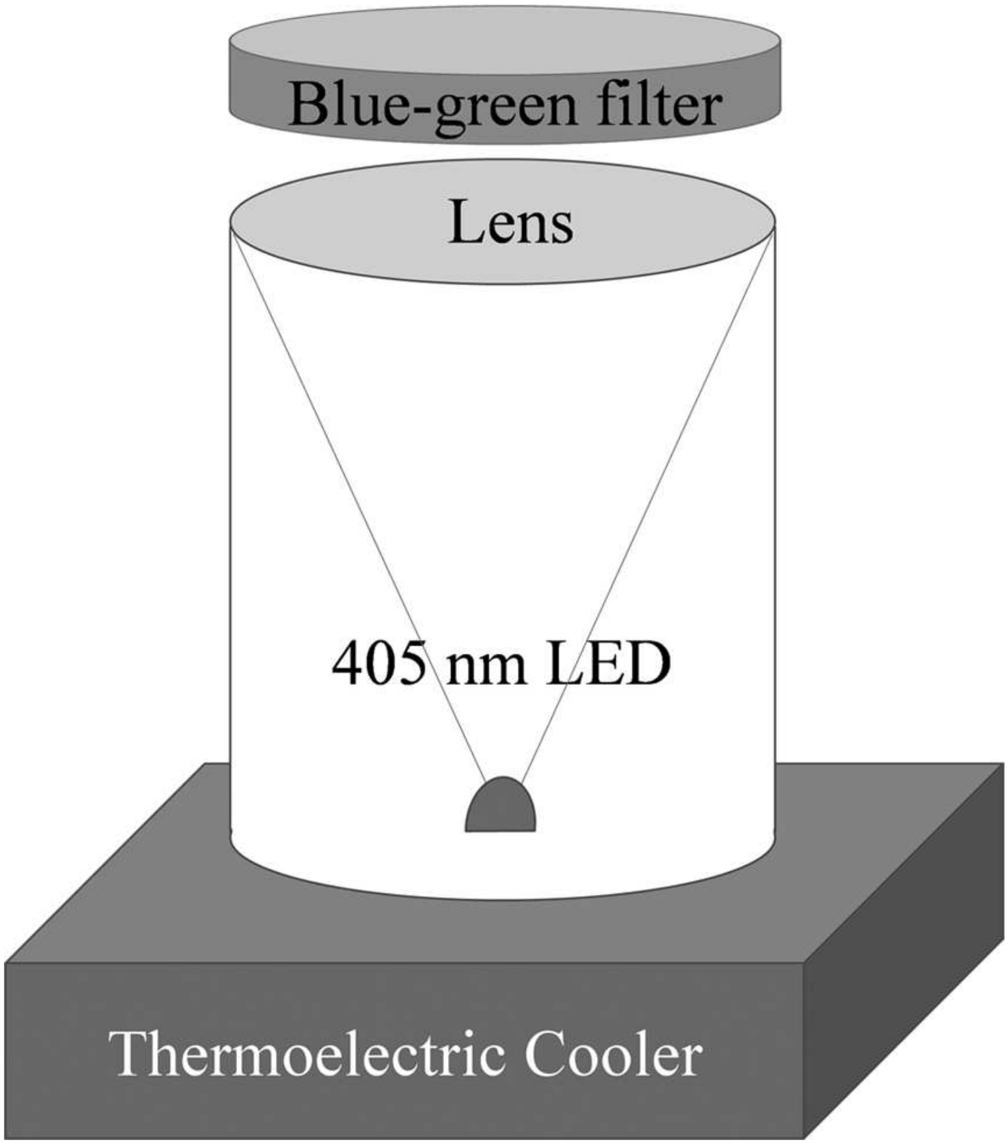

72x82mm (300 x 300 DPI)

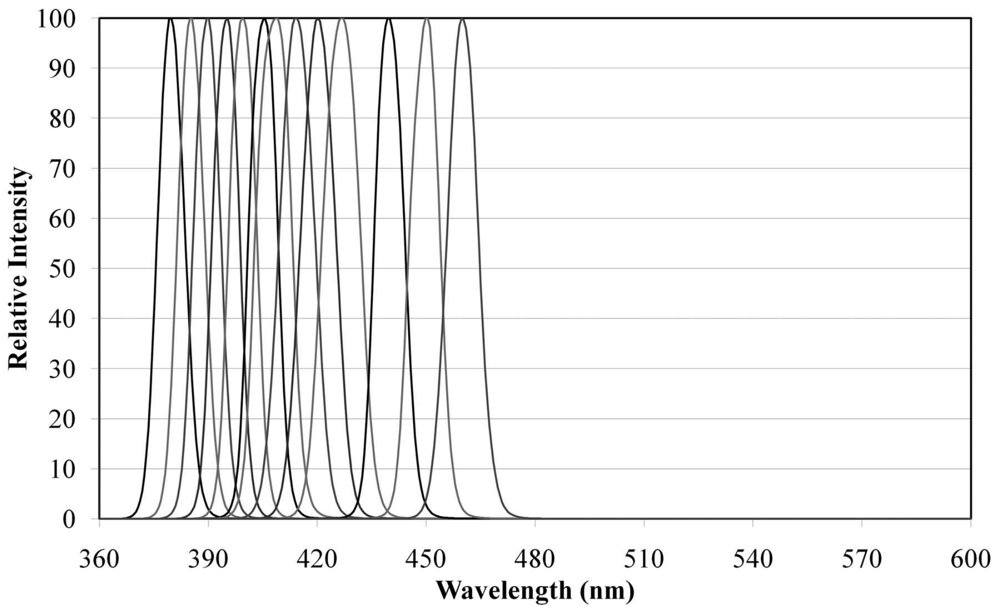

152x92mm (300 x 300 DPI)

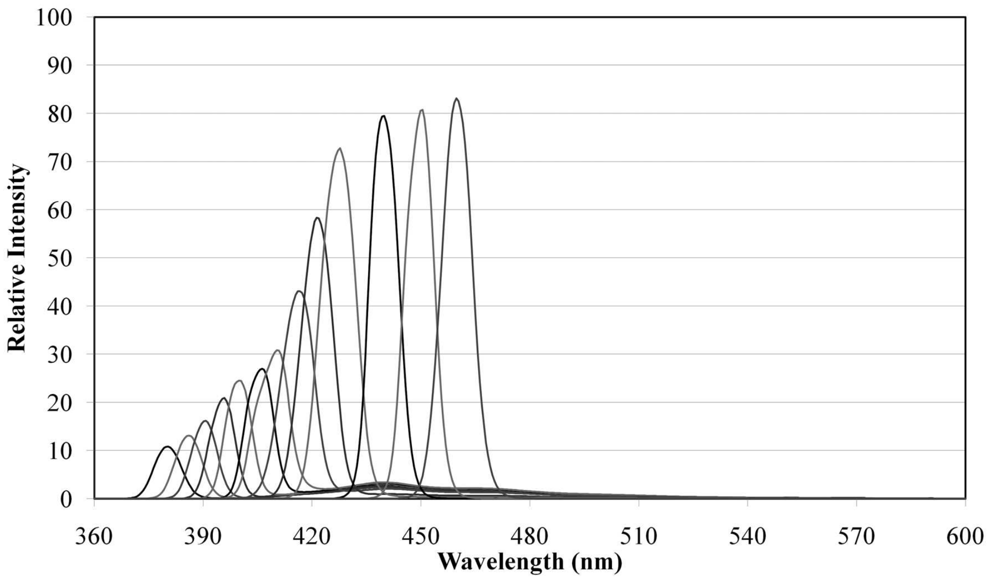

152x87mm (300 x 300 DPI)

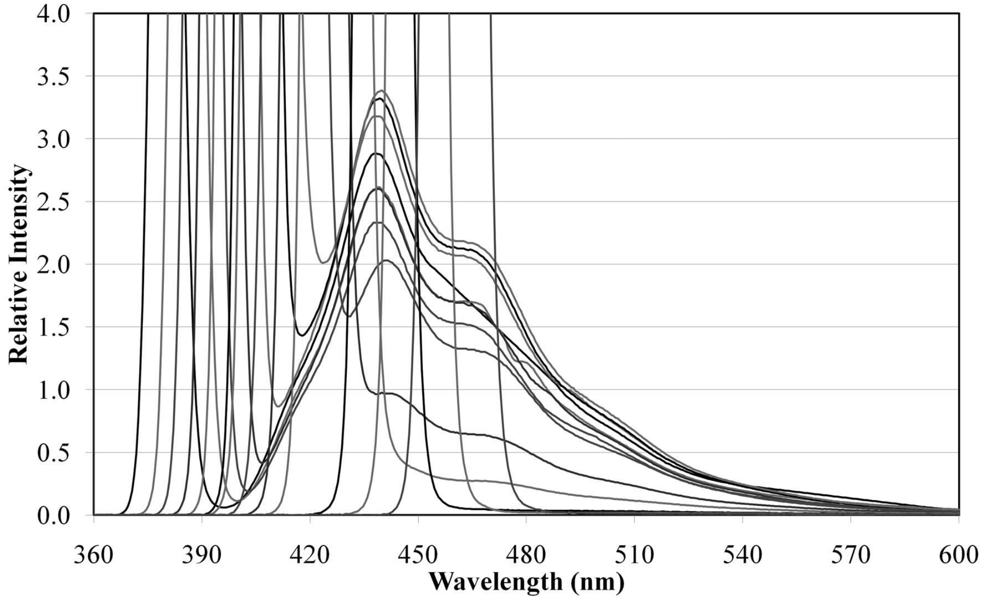

152x91mm (300 x 300 DPI)

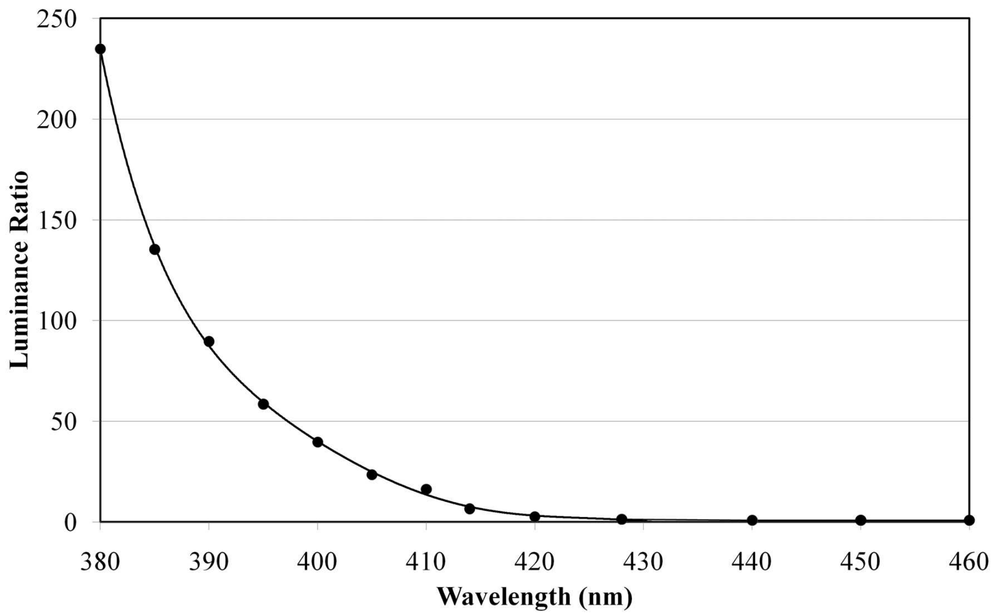

152x93mm (300 x 300 DPI)

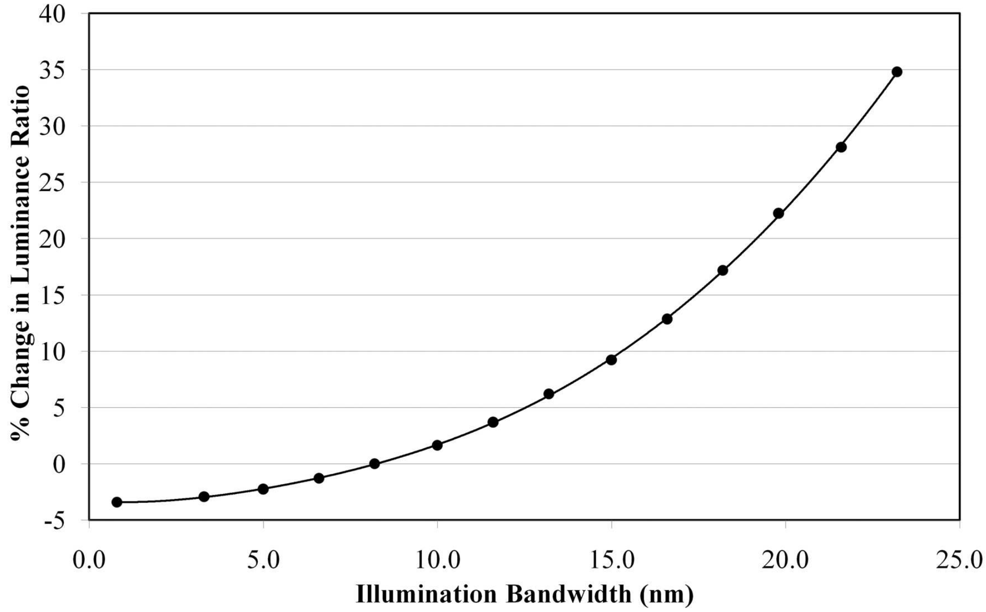

152x93mm (300 x 300 DPI)

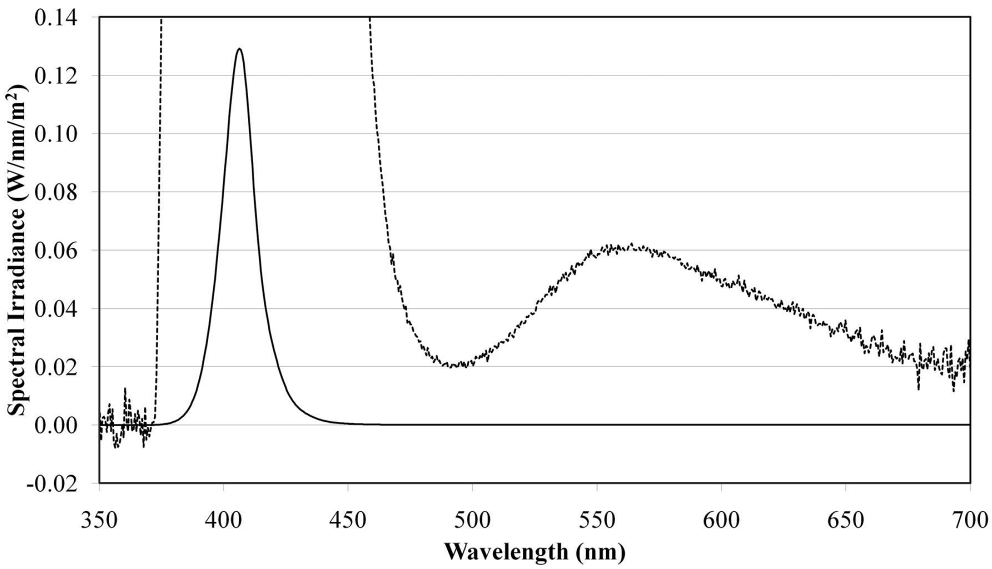

152x86mm (300 x 300 DPI)

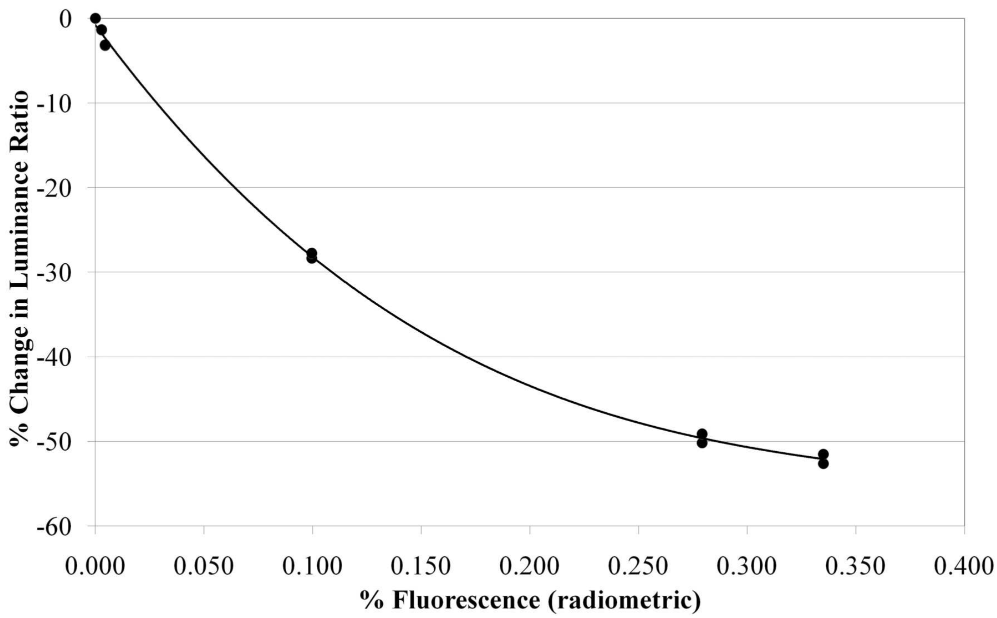

152x93mm (300 x 300 DPI)

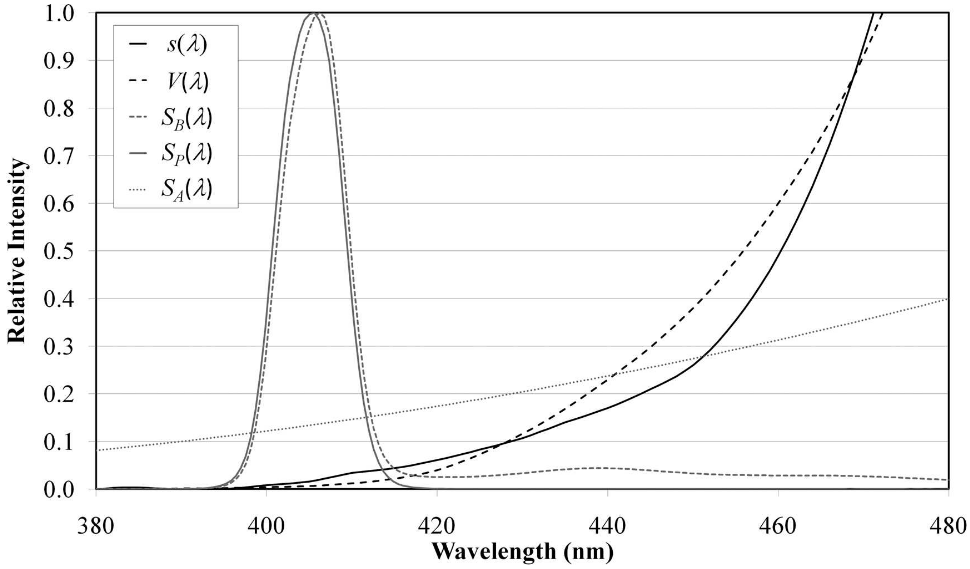

152x87mm (300 x 300 DPI)

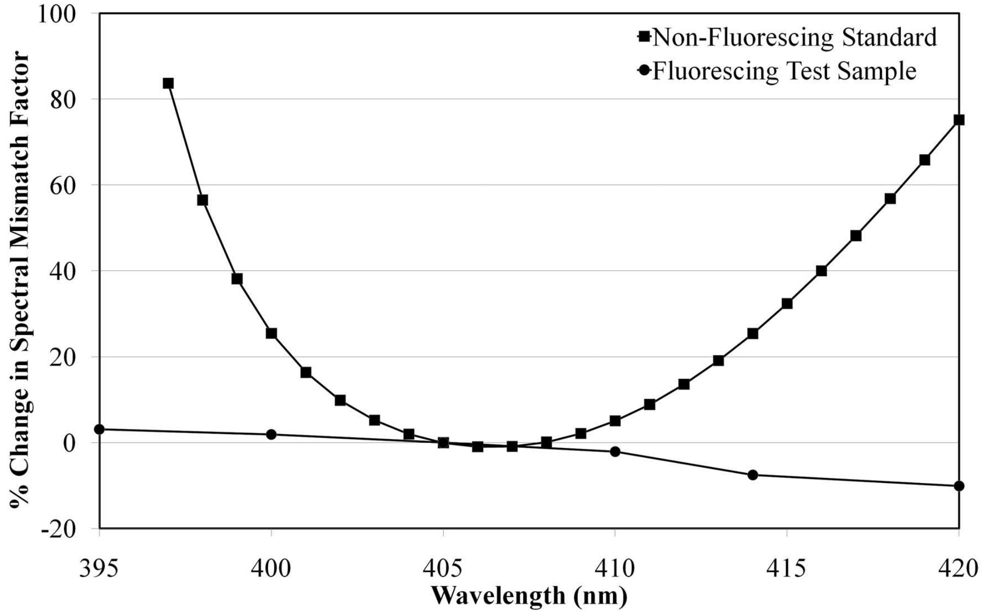

152x93mm (300 x 300 DPI)

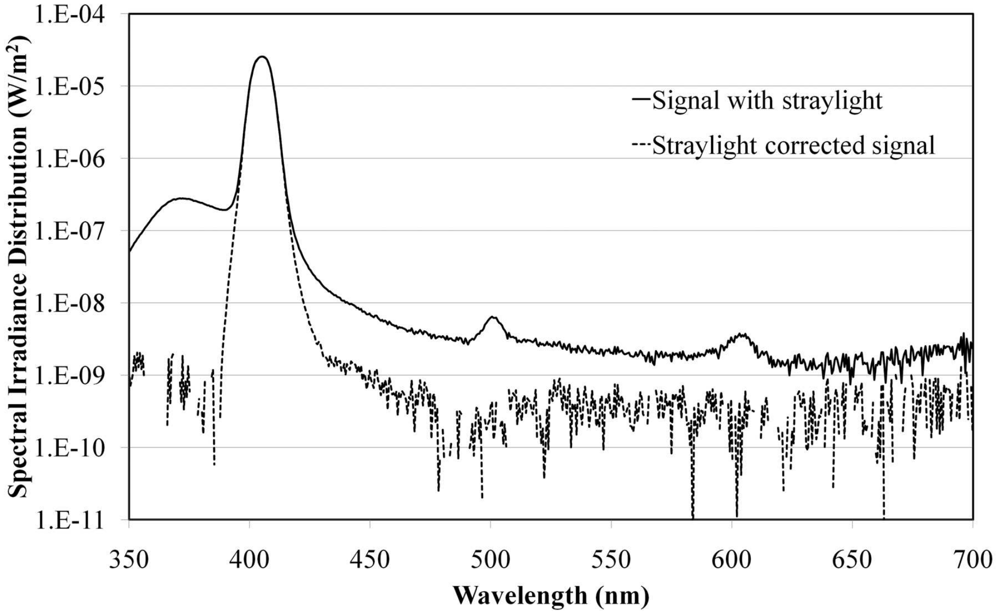

152x93mm (300 x 300 DPI)

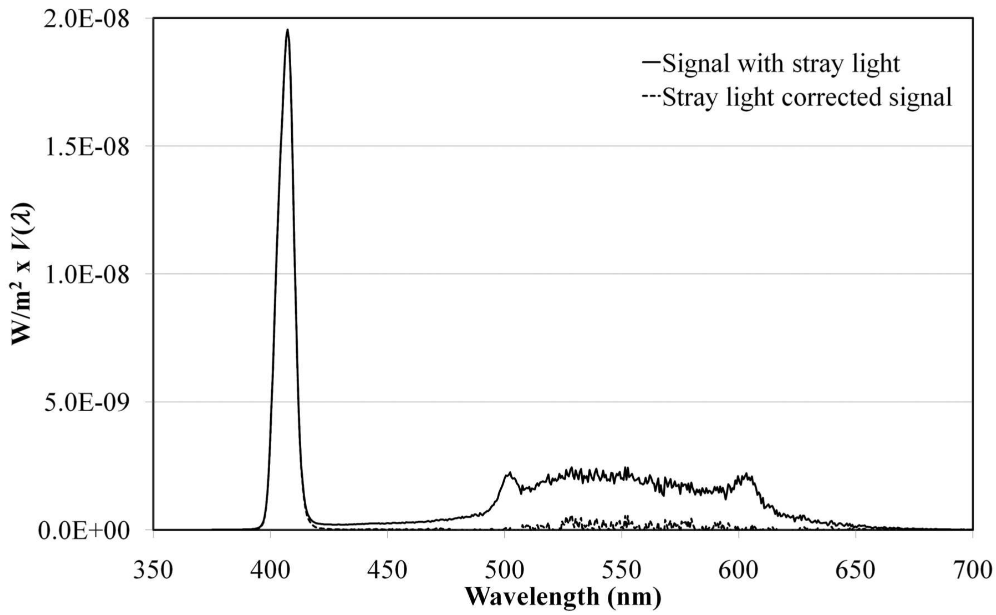

152x93mm (300 x 300 DPI)

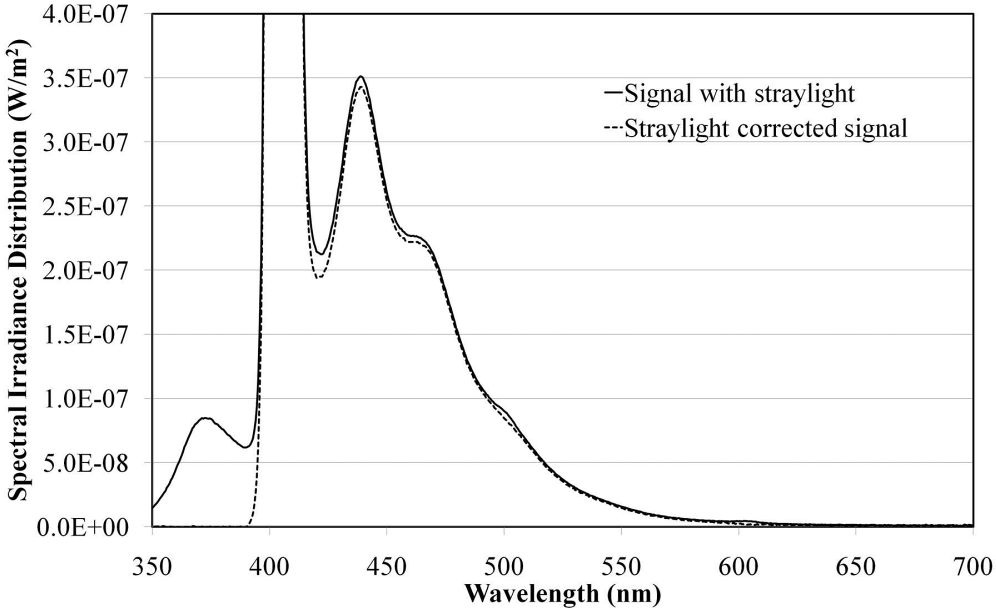

152x93mm (300 x 300 DPI)

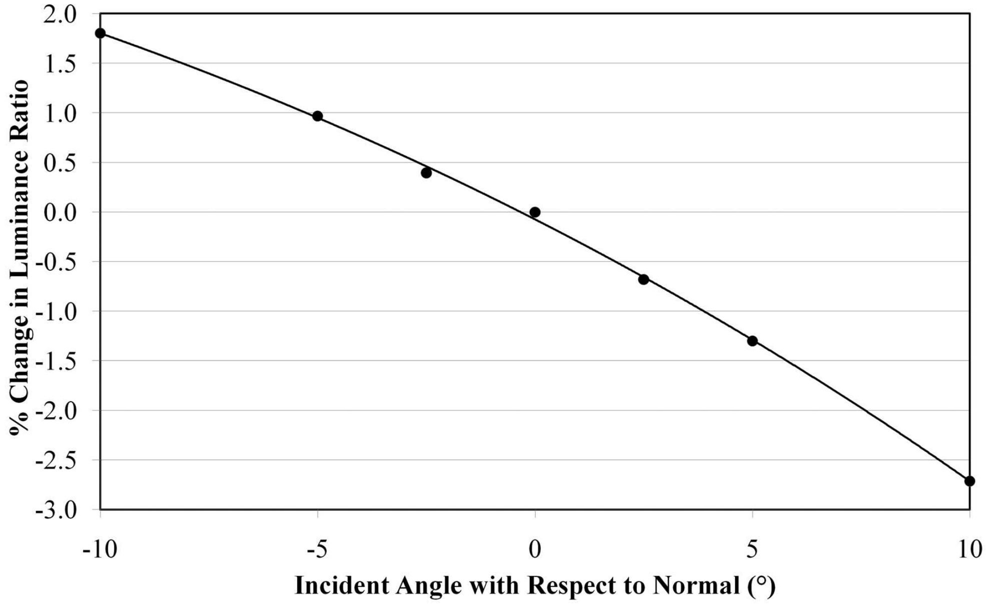

152x93mm (300 x 300 DPI)

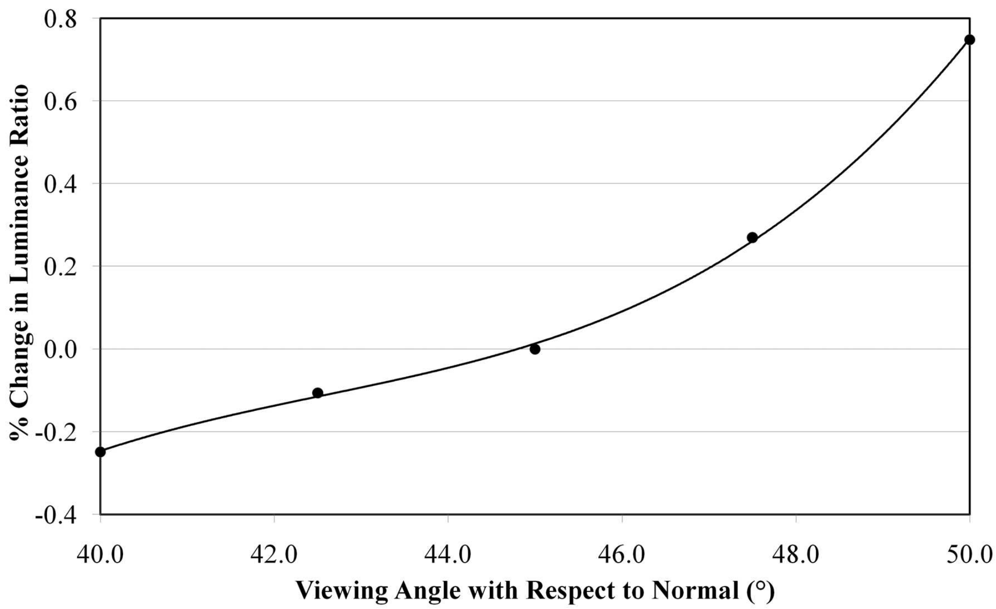

152x93mm (300 x 300 DPI)